Demonstration of an O-band InP Monolithically Integrated 4x4 SOA-based Broadcast and Select Optical Space Switch

Marijn Rombouts(1), Aref Rasoulzadeh Zali(1), Stefanos Andreou(2), Steven Kleijn(2), Nicola Calabretta(1)

(1) Eindhoven University of Technology and Eindhoven Hendrik Casimir Institute, PO Box 513, 5600 MB Eindhoven, The Netherlands m.p.g.rombouts@tue.nl
(2) SMART Photonics, High Tech Campus 29, 5656 AE Eindhoven, The Netherlands

Abstract *An O-band photonic integrated 4x4 SOA-based space switch based on the broadcast and select architecture has been designed and fabricated. Experimental validation shows error-free operation with a power penalty of $<$ 0.5 dB, an on/off ratio of 40 dB and an OSNR of 50 dB.*

Introduction

Machine learning clusters and artificial intelligence (AI) training have become increasingly popular in recent years. The recent introduction of OpenAI's ChatGPT made large-scale models available to the public, which enables the integration of AI in everyday objects and tasks. As a result, the model scale is doubling yearly, causing a proportional increase in the overall model size[1]. These developments require a highly efficient and scalable compute infrastructure.

Today's AI accelerators have multi-Tb/s interfaces[2] to share intermediate data for distributed training, generating large traffic flows. Throughput and latency are important network characteristics to avoid unnecessary computation stalls causing the overall training time to increase. With the recent developments in terms of co-packaged optics (CPO)[3], compute cores can now be directly attached to the network. Interface bottlenecks can be fully removed by combining CPOs with flat, all-optical networks such as OPSquare (Fig. 1a)[4],[5]. An important component in such network are the optical switches, which allows optical traffic flows to be redirected dynamically. Transparent optical operation allows the network to be upgraded in terms of data rate, modulation format and wavelength grid without having to replace the optical switches. Furthermore, the lack of an O/E/O conversion reduces power consumption compared to the electronic counterparts and reduces the amount of costly (pluggable) optical transceivers.

There is a large variety in optical switches, ranging from bulky, free-space MEMS-based switches[6] down to small photonic integrated devices. Integrated switches allow for many optical functions on a small surface, combined with the potential of economic mass-manufacturing.

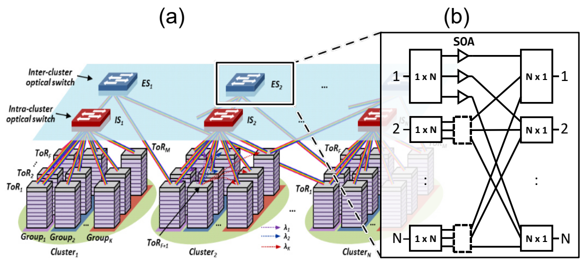

Fig. 1: (a) A flat optical network called OPSquare[4] where SOA-based switches are used. (b) The broadcast and select architecture, where input signal is split by N, selected using an SOA and combined to the output port.

Many integrated optical switches operate in the C-band, only a few O-band switches have been presented[7]–[10]. O-band switches are important to maintain compatibility and increase the chance of adoption in current data center environments. The O-band is favored for its low fiber dispersion, allowing for low-complexity, low-cost and efficient interconnects without the need for digital signal processors (DSPs). The higher fiber loss is of negligible importance given the relatively short fiber lengths of up to hundreds of meters.

With bigger and bigger networks, switch radii need to grow along. Common switch topologies based on 2x2 Mach-Zehnder Interferometer (MZI) building blocks face large optical losses, often in the order of 5 to 15 dB fiber-to-fiber loss for a switch radix of 8[7],[8],[11]. Since optical power budgets are tight, it is important to strive towards a zero loss device. The insertion loss can be reduced by using semiconductor optical amplifiers (SOAs) as a switching element in the 2x2 building blocks[10], achieving a zero fiber-to-fiber insertion loss. However, SOAs add noise, decreasing the optical signal-to-noise ratio (OSNR) of the optical signals[12] and therefore limiting the ideal channel capacity. Common switch topologies such as Benes, PILOSS and crossbar require more cascaded (SOA) elements for larger switch radii, further degrading the OSNR. Multicasting operation

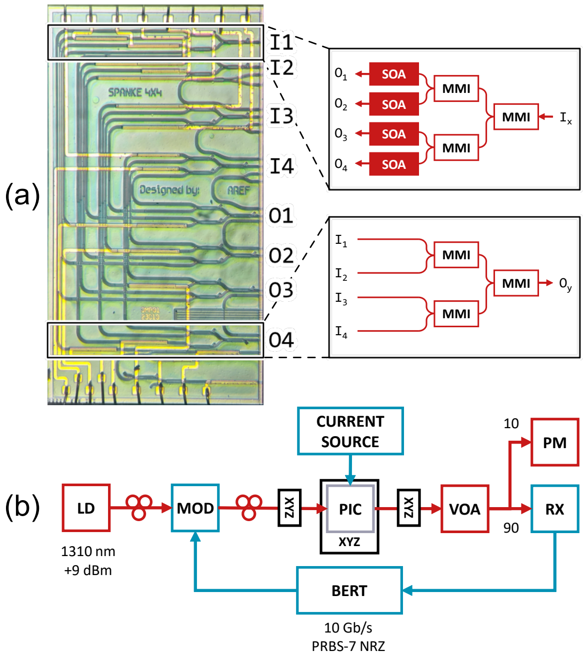

Fig. 2: (a) Photograph of the fabricated 4x4 optical switch. The inset shows a simplified version of the broadcast and select architecture for any input port $\mathtt{I}_x$ and output port $\mathtt{O}_y$. (b) Transmission measurement setup.

is naturally supported with no extra losses.

The broadcast and select topology (Fig. 1b) is strictly non-blocking and uses SOAs as switching elements. Only a single SOA per optical path is required, limiting the total OSNR degradation whilst providing gain to compensate for the on-chip losses. Nanosecond switching speeds of SOAs have been demonstrated, reducing port down-time. Furthermore, its high on/off ratio is beneficial for larger switch radii, where crosstalk is limiting performance.

In this paper we present the design, fabrication and characterization of the first monolithically integrated O-band 4x4, SOA-based broadcast and select and wavelength agnostic switch. The design of the photonic integrated circuit (PIC) is discussed and its performance is experimentally validated. With an OSNR of 50 dB, error-free operation is demonstrated at 10 Gb/s with an average receiver power penalty of 0.4 dB and an on/off ratio up to 40 dB.

Design and fabrication

The switch topology is based on a broadcast and select or Spanke architecture, as shown in Fig. 2a. The input signal is split by two cascaded 2x2 multimode interference couplers (MMIs) to four paths. Each path is equipped with an SOA to block or pass the optical signal. All passed signals are looped back towards a second set of two cascaded 2x2 MMIs to be combined for the output port. Coupling light in and out of the PIC happens on the east-side using edge-couplers. The electrical pads for the SOAs are located on the north and south-side of the PIC. The SOAs have lengths between 350 and 650 μm, to evaluate the impact on its optical characteristics.

The switch is designed using Nazca Design and the open-access O-band PDK of SMART Photonics. The design uses the active-passive integration platform to integrate quantum well SOAs[13], the 2x2 MMIs[14] and the waveguide structures. First, the active layer stack is epitaxially grown on a 3-inch wafer with an n-type InP substrate. The active components are defined, after which the passive layers are regrown. The waveguides are etched using an inductively coupled plasma (ICP) dry etching process. At last, the waveguides are passivated and planarized through the deposition of a Polyimide layer. All growth and processing steps are performed by SMART Photonics. The fabricated chip is shown in Fig. 2a.

Experimental setup and results

The 2 x 4.6 mm^2 PIC is glued onto a water-cooled aluminium chuck which is set to 20 ℃. Light is coupled using two lensed fibers. For all static experiments, the setup consist of the 1310 nm laser diode, a variable optical attenuator to control the laser power into the chip, a polarization controller to rotate the signal to the quasi-TE mode and an optical power meter. Alternatively, an optical spectrum analyzer is used. A constant current source drives the SOAs.

First, the IV-curves in Fig. 3a show typical diode characteristics for all 16 SOAs with a forward voltage of 1.4 to 1.7 V at 100 mA. A 376 μm and 550 μm SOA between output 2 (O2) and input 4 (I4) and I1 and O2, respectively, are highlighted. Simultaneously, the cumulative amplified spontaneous emission (ASE) power has been measured at both output ports, shown in Fig. 3b. From 50 mA, the optical power saturates. A small difference of 1.3 dB is measured between the two ports, as the SOA is located closer to I4 than to O2. By sweeping the drive current from 10 to 100 mA, the ASE spectra are recorded. Fig. 3c shows that the peak shifts from 1302 to 1281 nm with increasing current due to the band-filling effect. The 376 μm SOA gain at 1310 nm is calculated in Fig. 3d, by assuming an MMI insertion loss of 3.5 dB[14] and edge-coupler to fiber coupling loss of 5 dB. The in and output powers are the fiber powers. At 10 mA, the SOA is trans-

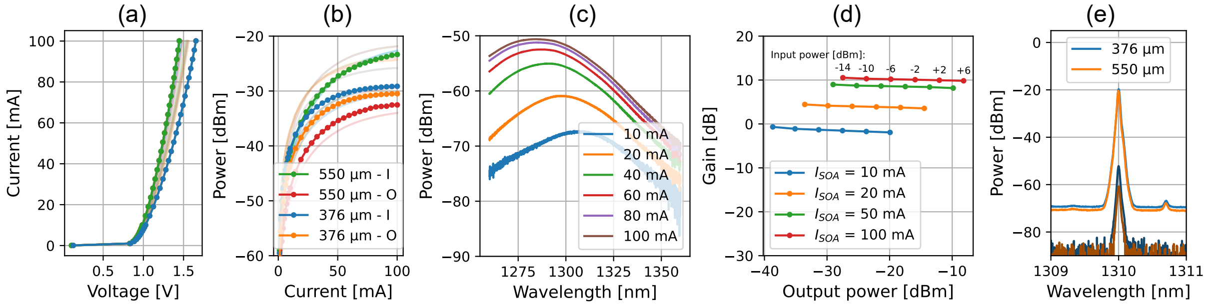

Fig. 3: (a) Current-voltage (IV) relation. All SOAs are included in a light shaded colour. (b) Cumulative output power measured at the in and output ports. The light shaded colours indicate all other SOAs, measured at the input ports. (c) ASE spectra for various drive currents for the 376 μm SOA. (d) Gain versus output power for various drive currents for the 376 μm SOA. The input power is indicated per point and holds for all values of I_{SOA}. (e) On/Off ratio of 40.3 dB for a 550 μm SOA and 32.3 dB for a 376 μm SOA

parent, and the maximum gain saturates around 10 dB. The input power has negligible effects on the gain, as the laser power is not enough to saturate the SOA with an approximate maximum on-chip SOA input power of -6 dBm. The on-chip losses cannot be compensated at 1310 nm, resulting in an insertion loss of -4 dB. Given the 5 dB power difference in the ASE curves in Fig. 3c between the gain peak at 1280 nm and this gain at 1310 nm, operating at a lower wavelength could result in lossless operation. Unfortunately, such laser was not available at the time of the experiments. The scalability of the topology has already been demonstrated using a single discrete SOA[12]. By employing longer SOAs and the addition of a booster SOA, a switch radix of 32 or even 64 is feasible at a cost of a degraded OSNR. However, other topologies would require at least 3 SOAs for an 8x8 configuration. Another advantage of SOA-based switches is the high on/off ratio. Fig. 3e shows the spectrum in the on and off state of the long and short SOA, with an isolation of 40.3 dB at an SOA length of 550 μm. The lowest measured on/off ratio is 32.3 dB for the 376 μm SOA.

Fig. 2b shows the experimental setup for the transmission experiments. A 10 Gb/s bit error rate tester (BERT) generates a pseudo-random bit sequence (PRBS-7) and is connected to an external Mach-Zehnder modulator (MZM). Polarization controllers are used to maintain the TE mode in the MZM and PIC. At the output, an optical attenuator is connected to a 90/10 splitter to measure the optical power and pass the signal to an avalanche photodiode (APD) receiver with a high sensitivity of -28 dBm.

The OSNR is shown in Fig. 4a for various optical input powers and SOA drive currents. The OSNR ranges from 30 to 50 dB, proportional to the input power, and the drive current seems to be of negligible impact on the OSNR. The bit error rate (BER) curves are shown in Fig. 4b. The I4 - O2 path is shown twice in two propagation directions. All ports connected to O2 are measured, except for I3 due to a damaged facet. The drive current of the SOAs are set to 100 mA. At 10^{-9}, i.e. error-free, the power penalty across the measured optical paths varies between 0.3 and 0.5 dB. The power penalty difference in propagation direction is negligible (0.1 dB). The eyes, inset in Fig. 4b, are wide open and show no bandwidth limiting effects or distortion besides noise.

Conclusions

We have designed and experimentally demonstrated a monolithically integrated 4x4 SOA-based broadcast and select switch in InP, operating in the O-band. Error-free performance has been demonstrated at 10 Gb/s with a maximum power penalty of 0.4 dB. OSNR up to 50 dB and on/off ratios beyond 40 dB are measured, allowing for transmission with minimal added noise and crosstalk. The switch demonstrates performance ideal for high-capacity and low-cost data center interconnects.

Acknowledgements

This work has been partially supported by the EU research and innovation program ADOPTION grant agreement 101070178 and ALLEGRO grant agreement 101092766.

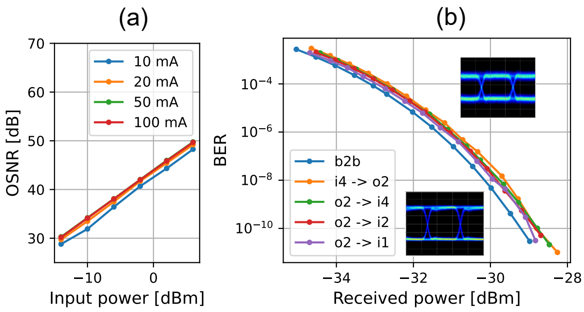

Fig. 4: (a) The SOA OSNR at 1310 nm for various drive currents. (b) BER curves for various optical paths. The insets show the eye diagrams of the b2b curve (bottom) and the I4 - O2 path (top).

References

[1] J. Sevilla, L. Heim, A. Ho, T. Besiroglu, M. Hobbhahn, and P. Villalobos, *Compute Trends Across Three Eras of Machine Learning*, arXiv:2202.05924 [cs], Mar. 2022. DOI: 10.48550/arXiv.2202.05924. [Online]. Available: http://arxiv.org/abs/2202.05924.

[2] *NVIDIA H100 Tensor Core GPU Architecture*, 2022.

[3] K. Hosseini, E. Kok, S. Y. Shumarayev, *et al.*, "8 Tbps Co-Packaged FPGA and Silicon Photonics Optical IO", en, p. 3, 2021.

[4] F. Yan, W. Miao, O. Raz, and N. Calabretta, "Opsquare: A flat DCN architecture based on flow-controlled optical packet switches", *Journal of Optical Communications and Networking*, vol. 9, no. 4, pp. 291–303, Apr. 2017, Conference Name: Journal of Optical Communications and Networking, ISSN: 1943-0639. DOI: 10.1364/JOCN.9.000291.

[5] M. P. G. Rombouts and N. Calabretta, "On the Performance of a Fast Optically Switched Network for Machine-Learning Accelerator Clusters", EN, in *Optical Fiber Communication Conference (OFC) 2023 (2023), paper W1G.3*, Optica Publishing Group, Mar. 2023, W1G.3. [Online]. Available: https://opg.optica.org/abstract.cfm?uri=OFC-2023-W1G.3.

[6] R. Urata, H. Liu, K. Yasumura, *et al.*, "Mission Apollo: Landing Optical Circuit Switching at Datacenter Scale", en, p. 13, Aug. 2022.

[7] J. Faneca, T. D. Bucio, F. Y. Gardes, and A. Baldycheva, "O-band N-rich silicon nitride MZI based on GST", en, *Applied Physics Letters*, vol. 116, no. 9, p. 093 502, Mar. 2020, ISSN: 0003-6951, 1077-3118. DOI: 10.1063/1.5140350. [Online]. Available: https://pubs.aip.org/aip/apl/article/38513.

[8] N. Dupuis, J. E. Proesel, N. Boyer, *et al.*, "An 8ã8 Silicon Photonic Switch Module with Nanosecond-Scale Reconfigurability", in *2020 Optical Fiber Communications Conference and Exhibition (OFC)*, Mar. 2020, pp. 1–3.

[9] K. Suzuki, R. Konoike, G. Cong, *et al.*, "Strictly Non-Blocking 8 ã 8 Silicon Photonics Switch Operating in the O-Band", *Journal of Lightwave Technology*, vol. 39, no. 4, pp. 1096–1101, Feb. 2021, Conference Name: Journal of Lightwave Technology, ISSN: 1558-2213. DOI: 10.1109/JLT.2020.3024016.

[10] H. R. Mojaver, V. Tolstikhin, B. Gargallo, *et al.*, "8 ã 8 SOA-based optical switch with zero fiber-to-fiber insertion loss", en, *Optics Letters*, vol. 45, no. 16, p. 4650, Aug. 2020, ISSN: 0146-9592, 1539-4794. DOI: 10.1364/OL.399415. [Online]. Available: https://opg.optica.org/abstract.cfm?URI=ol-45-16-4650.

[11] K. Suzuki, R. Konoike, S. Suda, *et al.*, "Low-Loss, Low-Crosstalk, and Large-Scale Optical Switch Based on Silicon Photonics", en, *Journal of Lightwave Technology*, vol. 38, no. 2, pp. 233–239, Jan. 2020, ISSN: 0733-8724, 1558-2213. DOI: 10.1109/JLT.2019.2934768. [Online]. Available: https://ieeexplore.ieee.org/document/8794739/.

[12] M. P. G. Rombouts and N. Calabretta, "Scalability Assessment of O-band SOA-based Broadcast and Select Switch with 100 Gb/s LWDM Commercial Transceivers", EN, in *Optical Fiber Communication Conference (OFC) 2023 (2023), paper Th3D.3*, Optica Publishing Group, Mar. 2023, Th3D.3. [Online]. Available: https://opg.optica.org/abstract.cfm?uri=OFC-2023-Th3D.3.

[13] J. Hazan, S. Andreou, D. Pustakhod, S. Kleijn, K. A. Williams, and E. A. J. M. Bente, "1300 nm Semiconductor Optical Amplifier Compatible With an InP Monolithic Active/Passive Integration Technology", *IEEE Photonics Journal*, vol. 14, no. 3, pp. 1–11, Jun. 2022, Conference Name: IEEE Photonics Journal, ISSN: 1943-0655. DOI: 10.1109/JPHOT.2022.3175373.

[14] J. Hazan, D. Pustakhod, S. Kleijn, S. Andreou, K. A. Williams, and E. A. Bente, "Broadband multimode interference coupler on InP substrate with flat wavelength response over the whole O-band", in *2021 IEEE Photonics Conference (IPC)*, ISSN: 2575-274X, Oct. 2021, pp. 1–2. DOI: 10.1109/IPC48725.2021.9592858.